State estimation of an electro-pneumatic gearbox actuator

Adam Szabo * **Tamas Becsi** * **Peter Gaspar** ** **Szilard Aradi** *

* *Department of Control for Transportation and Vehicle Systems*
Budapest University of Technology and Economics
Budapest, Hungary
[szabo.adam;becsi.tamas;aradi.szilard]@mail.bme.hu
** *Computer and Automation Research Institute*
Hungarian Academy of Sciences
Budapest, Hungary
gaspar.peter@sztaki.mta.hu

Abstract: This paper presents two state estimator algorithms, a Kalman and an Extended Kalman filter in order to determine the chamber pressures of a pneumatic actuator without the application of pressure sensors. The presented state estimators were validated against laboratory measurements, then it was shown, that in applications with high computational resources, such as simulations both algorithms can provide acceptable results and they have nearly the same accuracy. Meanwhile, in embedded systems with higher realizable sample time the Kalman filter, which is based on the linearized state-space representation of the system, can not handle the nonlinear behavior of the actuator in every test case. Based on the validation results, a suggestion was made in order to further improve the accuracy of the presented methods.

Keywords: Pneumatic actuator, State observer, Kalman filter, Extended Kalman filter, Nonlinear system

1. INTRODUCTION

Pneumatically driven systems are widely used in industrial applications in order to achieve force transmission and to obtain accurate position control Saravanakumar et al. (2017). Researches connected to the vehicle industry mainly focus on the single- and double acting cylinders, which can be used in several systems, such as air brake systems Karthikeyan et al. (2011), and electro-pneumatic clutches Szimandl and Nemeth (2013a). Meanwhile, many of recent studies focus on the modeling and control of pneumatic muscle actuators, such as Hoovsk et al. (2016), Oliver-Salazar et al. (2017) and Doumit and Pardoel (2017).

They have several advantages over hydraulic and electromechanic actuators, such as low specific weight, high power density, and the unlimited supply of air, which can be easily stored and transported. However, predicting and controlling them can be complex, due to their nonlinear behavior Palomares et al. (2017). In literature a high variety of applicable control methods can be found, such as the linear quadratic control Szimandl and Nemeth (2009), sliding mode control Szimandl and Nemeth (2013b), H-infinity method Szimandl and Nemeth (2014) and Neural Network based controllers, such as Son et al. (2017), Chiang and Chen (2017), XiaoJun et al. (2006). In industrial and real-time applications, such as Mihaly et al. (2017), the most commonly used method is the PID control, which in order to control the nonlinear system should be enhanced through gain scheduling, or it should be used in cascaded control Saleem et al. (2015).

While PID controllers do not need detailed knowledge of the system, only a reference signal and its actual value, the scheduling of the controller parameters, or switching between different controllers is mostly triggered by other states of the system. In case of pneumatic systems these states are typically the actuation force and the piston velocity, therefore it would be evident to measure the velocity and the chamber pressures, though one of the main aspects of a product development is to keep the cost of the product low. As a consequence, the required states have to be calculated with acceptable accuracy, therefore the system can be controlled suitably and the its cost can be kept down.

The objective of the research is to design different state observers and to analyze their performances on measurement data.

The paper is organized as follows: Section 2 describes the tested actuator, Section 3 presents the developed state observers. Section 4 shows some conclusion remarks.

2. SYSTEM DESCRIPTION

The presented actuator is part of the automated manual transmission of a heavy duty vehicle. It sets the gearbox

to neutral, or shifts the proper gear inside a previously selected lane.

The cylinder is actuated by two 3-way 2-position solenoid valves. The valves can connect the chambers to the supply pressure, or release the air from them to the environment. There are three chambers within the actuator, two of them are working chambers (Chamber 1 and Chamber 2) and one is a control chamber. Both of the working chambers are connected to a single solenoid valve, while the control chamber serves as an air spring with no solenoid valve connected to its only port. The layout of the system can be seen in Fig. 1.
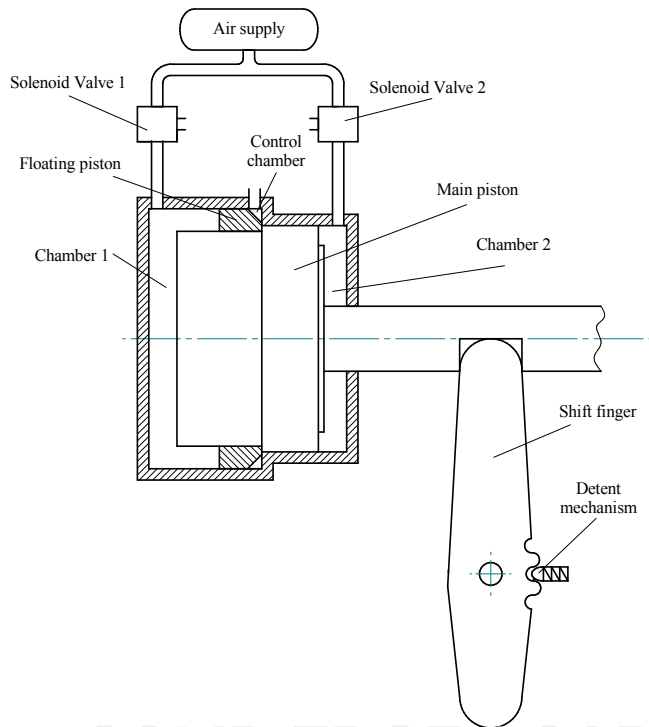

Fig. 1. Simplified layout of the gearbox actuator

Two pistons can be found within the cylinder, the main piston actuates the shift finger and through it, it moves the gear shift linkage and the synchronizer sleeve, hence it can shift between different gears. It has three dedicated positions: two gears (High and Low end positions of the piston) and Neutral position. Its movement is generated by the opposing pressure forces inside the working chambers. The floating piston either helps, or acts against the movement of the main piston through collision, meanwhile it tunes the volume of the control chamber.

The observed system contains only a position sensor, but to validate the developed estimators the chamber pressures also had to be measured.

3. STATE OBSERVER DEVELOPMENT

In order to reduce the cost of the system, the chamber pressures cannot be measured, thus they need to be calculated to achieve accurate control. The layout of the controlled system can be seen in Fig. 2. In this research, two state observers were developed and validated against laboratory measurement, while the aim of a future research will be the development of a state observer based controller.
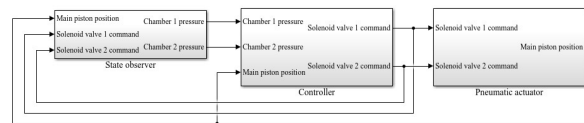

Fig. 2. Simplified layout of the controlled system

First, a Kalman filter was developed to examine if the system behavior can be estimated with a linearized state-space representation. Then, an extended Kalman filter was presented, which contains nonlinear equations used in Szabo et al. (2018b) to describe the model of the system. The covariance of the process noise Q is calculated based on the results of the model validation presented in the previous research, the covariance of the observation noise R describes the accuracy of the position sensor.

3.1 Measurement

The measurement was made on a standalone gearbox actuator, which was connected to 9.5bar supply pressure and was driven by direct solenoid valve commands. The measured signals were the following:

- Supply pressure
- Solenoid valve 1 command
- Solenoid valve 2 command
- Chamber 1 pressure
- Chamber 2 pressure
- Main piston position

The signals were measured with CANape via XCP protocol. The supply and chamber pressures were measured with 2ms sample time, while the sample time of the solenoid valve commands and the main piston position was 5ms.

The measured test cases contained four different test cases, according to the typical operation cases of the system, which are the following: from Neutral to High, from High to Neutral, from Neutral to Low and from Low to Neutral gear changes. In the following sections, the results of the state observer development will be presented for the last two test cases.

3.2 Kalman-filter

Kalman-filter (KF) algorithm can be divided into two distinct phases: a prediction (a priori) state, which uses the state estimation from the previous time step to estimate the current state, while the update (a posteriori) state refines the estimation with the current observation information.

The state space representation used in the Kalman filter is based on the one presented in Szabo et al. (2018a), where it was assumed, that all of the required signals can be measured, therefore in this application it had to be augmented with additional states. The modified state vectors are the following:
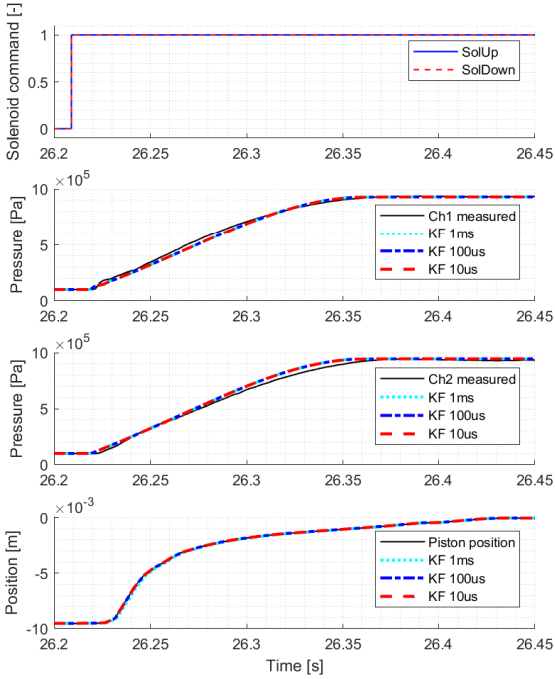
Fig. 3. State estimation with Kalman filter, Low to Neutral gear change

$$\underline{x} = \begin{bmatrix} p_{ch1} \\ p_{ch2} \\ m_{ch1} \\ m_{ch2} \\ x_{MP} \\ v_{MP} \end{bmatrix}, \quad \underline{y} = [x_{MP}], \quad \underline{u} = \begin{bmatrix} \dot{m}_{ch1} \\ \dot{m}_{ch2} \end{bmatrix} \quad (1)$$

The state state matrices can be described by multiple hybrid states based on the position of the main piston and state of the solenoid valves. One possible state of the matrices can be written as follows:

$$\underline{\underline{A}} = \begin{bmatrix} a_{11} & 0 & 0 & 0 & a_{15} & a_{16} \\ 0 & a_{22} & 0 & 0 & a_{25} & a_{26} \\ 0 & 0 & 0 & 0 & 0 & 0 \\ 0 & 0 & 0 & 0 & 0 & 0 \\ 0 & 0 & 0 & 0 & 0 & 1 \\ a_{61} & a_{62} & 0 & 0 & 0 & a_{66} \end{bmatrix} \quad (2)$$

$$\underline{\underline{B}} = \begin{bmatrix} b_{11} & 0 \\ 0 & b_{22} \\ 1 & 0 \\ 0 & 1 \\ 0 & 0 \\ 0 & 0 \end{bmatrix}, \quad \underline{C} = [0\ 0\ 0\ 0\ 1\ 0] \quad (3)$$

$$a_{11} = \frac{-\kappa_{air} A_{MP1} v_{MP}}{V_{ch1}} \quad (4)$$

$$a_{15} = \frac{\kappa_{air} A_{MP1}^2 v_{MP} p_{ch1} + k_{ht1} A_{ht1} A_{MP1}(T_{ch1} - T_{amb})}{V_{ch1}^2} \quad (5)$$

$$a_{16} = \frac{-\kappa_{air} A_{MP1} p_{ch1}}{V_{ch1}} \quad (6)$$

$$a_{22} = \frac{\kappa_{air} A_{MP2} v_{MP}}{V_{ch2}} \quad (7)$$

$$a_{25} = \frac{\kappa_{air} A_{MP2}^2 v_{MP} p_{ch2} + k_{ht2} A_{ht2} A_{MP2}(T_{ch1} - T_{amb})}{V_{ch2}^2} \quad (8)$$

$$a_{26} = \frac{\kappa_{air} A_{MP2} p_{ch2}}{V_{ch2}} \quad (9)$$

$$a_{61} = \frac{A_{MP1}}{m_{MP}}, \ a_{62} = \frac{-A_{MP2}}{m_{MP}}, \ a_{66} = \frac{-d_f}{m_M P} \quad (10)$$

$$b_{11} = \frac{\kappa_{air} R_{air} T_{sup}}{V_{ch1}}, \ b_{22} = \frac{\kappa_{air} R_{air} T_{sup}}{V_{ch2}} \quad (11)$$

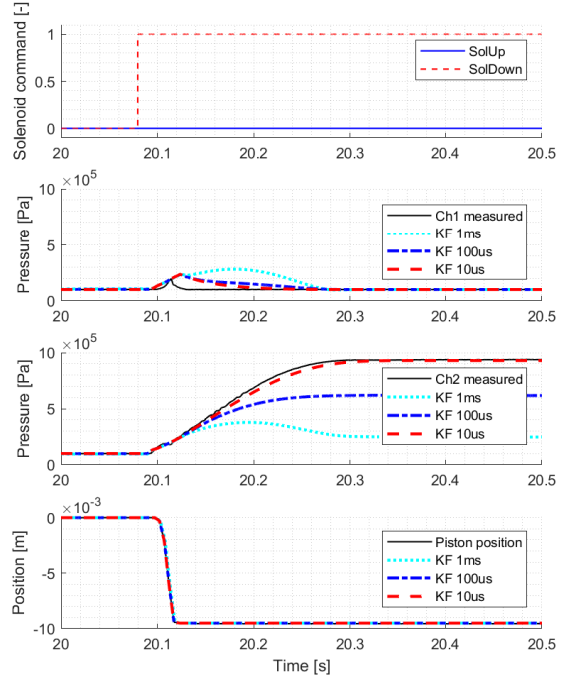Fig. 4. State estimation with Kalman filter, Neutral to Low gear change

where κ_{air} is the heat capacity ratio, R_{air} is the gas constant for air, V is the volume, p is the pressure, m is the air mass, T is the temperature, x is the position, v is the velocity, A is the area, k is the heat transfer coefficient, amb refers to ambient, sup refers to supply, $ch1$ refers to Chamber 1, $ch2$ refers to Chamber 2, MP refers to main piston, ht refers to heat transfer, $inw1$ and $inw2$ refers to the temperature of the air flowing to Chamber 1 and Chamber 2.

The given representation describes the system behavior in continuous time, hence it had to be discretized and the measurement signals had to be interpolated to match the sample time of the estimator. First, the sampling time was 0.01ms to analyze the model behavior, then it was increased to 1ms, which is a typical sample time in embedded system applications.

As an example, Fig. 3 shows a Low to Neutral gear change, where seemingly there is no difference between the pressures estimated with different methods and sample times and they are also corresponding to the measured signals. As the measured position has much higher reliability, than the model there is no perceptible difference between the measured and estimated positions.

Figures showing the observer performances should be interpreted as follows: the first diagram shows the solenoid valve commands, on the second diagram the chamber pressures are shown, the third diagram shows the main piston position signals.

In Fig. 4 a Neutral to Low gear change can be seen. Based on the second diagram (Chamber 1 pressure) it is assumable, that the speed estimation is inaccurate, thus the rate of the work term in the energy equation is overestimated, which possibly causes the increased difference between the measurement and calculation. On the third diagram (Chamber 2 pressure), it is shown, that with bigger sample times, the deviance of the state estimation also increases. Therefore, in this case the linearized equations can predict the model behavior only in case of 0.01ms sample time.

3.3 Extended Kalman-filter

The extended Kalman filter (EKF) uses nonlinear equations to predict the behavior of the system, hence in this application it should provide better results. The Low to Neutral gear change can be seen in Fig. 5, which shows that the pressure estimation is more accurate than in case of the Kalman filter.

Fig. 6. State estimation with extended Kalman filter, Neutral to Low gear change

these deviances were calculated, which can be seen in Table 1. As an example, deviances of Chamber 2 pressure in case of Low to Neutral gear change are shown in Fig 4, the conclusions made based on the figure are correct for both chamber pressures.
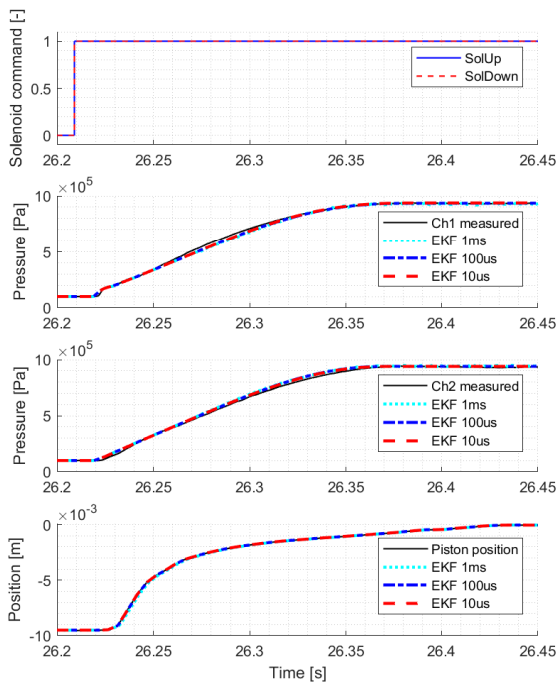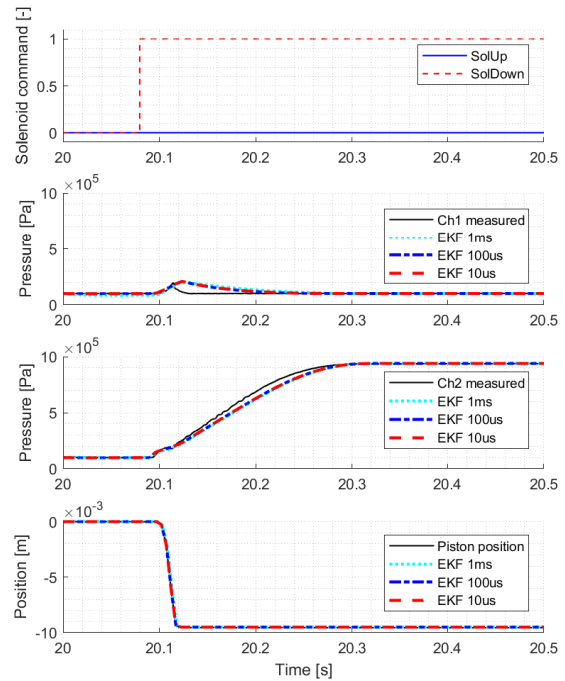

Fig. 5. State estimation with extended Kalman filter, Low to Neutral gear change

A Neutral to Low gear change can be seen in Fig 6. While the pressure deviance is for both chambers higher, than in case of Low to Neutral gear change, they still stay in an acceptable range compared to the Kalman filter.

4. CONCLUSION AND FUTURE WORK

For comparison purposes the deviance of the observers were plotted in each timestep, then the RMS values of
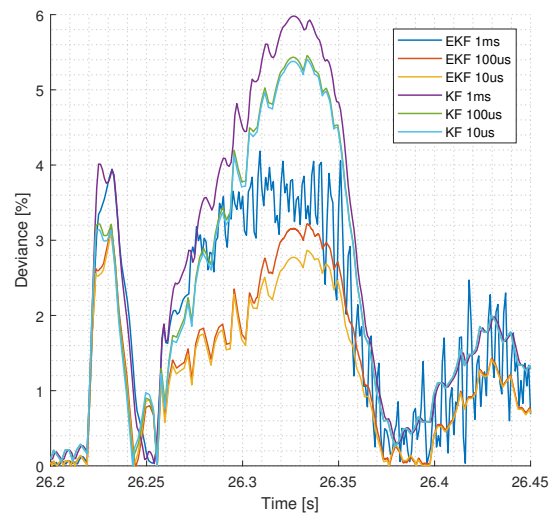

Fig. 7. Chamber 2 pressure deviances in case of Low to Neutral gear change

As it can be seen, in case of low to neutral gear change the difference between $10\mu s$ and $100\mu s$ sample times is negligible for both estimators and there is only a slight difference between the $100\mu s$ and 1ms simulations, while in case of equivalent sample times EKF provides better overall results compared to KF.

Table 1. RMS values of the pressure deviances

		EKF		KF	
		L to N	N to L	L to N	N to L
p_ch1	10 us	1.52	3.95	2.09	4.57
	100 us	1.49	3.88	2.06	5.50
	1 ms	1.62	4.53	1.77	12.15
p_ch2	10 us	1.62	4.18	2.87	3.21
	100 us	1.76	4.17	2.91	25.25
	1 ms	2.39	4.49	3.28	53.57

In case of Neutral to Low gear change, Kalman filter could achieve acceptable state prediction only with $10\mu s$ sample time, while the accuracy of the extended Kalman filter is similar to the previous test case.

In this paper two different state estimator algorithms have been presented through the application of a pneumatic gearbox actuator. The developed state estimators were compared to laboratory measurement and the results were analyzed.

It can be stated, that for simulation purposes, where the computational cost of the estimators is secondary, both algorithms are viable. However, in embedded systems where the resources are finite, only the nonlinear algorithm could provide state estimation with appropriate accuracy. Meanwhile, the developed algorithms have to be optimized for embedded applications, there is no significant difference between them regarding the computational cost.

To provide better results the accuracy of the speed estimation should also be examined, because it determines the estimated position (as its gradient) and it also affects the pressure estimation through the energy equation. Since the reliability of the measured position is much higher than the estimated position, the effect of the estimated speed on the observed position is negligible. However, it can decrease the accuracy of the pressure estimation when the mass flow rate of a chamber is small, thus the change of pressure is mostly caused by the movement of the piston, as it can be seen in Fig. 4.

As a first approximation, the piston velocity can be calculated by the numerical differentiation of the measured position signal. By comparing it to the estimated velocity, it can be stated, that the accuracy of the speed estimation is the worst. Because of the relative high sample time of the measurement, further development can not be done based on this approximation, in order to provide better overall estimation results, the measurement of the piston velocity and further tuning of its estimation is needed.

Further research will focus on the development of a closed loop system, where the estimated pressure signals will serve as an input of a controller. First, the developed controller will be tested in Model in the Loop environment, then it will be tested on the real system.

REFERENCES

Chiang, C.J. and Chen, Y.C. (2017). Neural network fuzzy sliding mode control of pneumatic muscle actuators. *Engineering Applications of Artificial Intelligence*, 65, 68 – 86. doi:https://doi.org/10.1016/j.engappai.2017.06.021.

Doumit, M.D. and Pardoel, S. (2017). Dynamic contraction behaviour of pneumatic artificial muscle. *Mechanical Systems and Signal Processing*, 91, 93 – 110. doi: https://doi.org/10.1016/j.ymssp.2017.01.001.

Hoovsk, A., Pite, J., idek, K., Tthov, M., Srosi, J., and Cveticanin, L. (2016). Dynamic characterization and simulation of two-link soft robot arm with pneumatic muscles. *Mechanism and Machine Theory*, 103, 98 – 116. doi: https://doi.org/10.1016/j.mechmachtheory.2016.04.013.

Karthikeyan, P., Chaitanya, C.S., Raju, N.J., and Subramanian, S.C. (2011). Modelling an electropneumatic brake system for commercial vehicles. *IET Electrical Systems in Transportation*, 1(1), 41–48. doi:10.1049/iet-est.2010.0022.

Mihaly, A., Baranyi, M., Nemeth, B., and Gaspar, P. (2017). Tuning of look-ahead cruise control in hil vehicle simulator. *Periodica Polytechnica Transportation Engineering*, 45.

Oliver-Salazar, M., Szwedowicz-Wasik, D., Blanco-Ortega, A., Aguilar-Acevedo, F., and Ruiz-Gonzlez, R. (2017). Characterization of pneumatic muscles and their use for the position control of a mechatronic finger. *Mechatronics*, 42, 25 – 40. doi: https://doi.org/10.1016/j.mechatronics.2016.12.006.

Palomares, E., Nieto, A., Morales, A., Chicharro, J., and Pintado, P. (2017). Dynamic behaviour of pneumatic linear actuators. *Mechatronics*, 45, 37 – 48. doi: https://doi.org/10.1016/j.mechatronics.2017.05.007.

Saleem, A., Taha, B., Tutunji, T., and Al-Qaisia, A. (2015). Identification and cascade control of servo-pneumatic system using particle swarm optimization. *Simulation Modelling Practice and Theory*, 52, 164 – 179. doi:https://doi.org/10.1016/j.simpat.2015.01.007.

Saravanakumar, D., Mohan, B., and Muthuramalingam, T. (2017). A review on recent research trends in servo pneumatic positioning systems. *Precision Engineering*, 49, 481 – 492. doi: https://doi.org/10.1016/j.precisioneng.2017.01.014.

Son, N.N., Kien, C.V., and Anh, H.P.H. (2017). A novel adaptive feed-forward-pid controller of a scara parallel robot using pneumatic artificial muscle actuator based on neural network and modified differential evolution algorithm. *Robotics and Autonomous Systems*, 96, 65 – 80. doi:https://doi.org/10.1016/j.robot.2017.06.012.

Szabo, A., Becsi, T., Gaspar, P., and Aradi, S. (2018a). Control design of an electro-pneumatic gearbox actuator. In *2018 14th IEEE/ASME International Conference on Mechatronic and Embedded Systems and Applications (MESA)*, 1–6. doi:10.1109/MESA.2018.8449145.

Szabo, A., Becsi, T., Gaspar, P., and Aradi, S. (2018b). Control oriented modeling of an electro-pneumatic gearbox actuator. In *2018 16th European Control Conference (ECC)*, 1–6.

Szimandl, B. and Nemeth, H. (2009). Closed loop control of electro-pneumatic gearbox actuator. In *2009 European Control Conference (ECC)*, 2554–2559. doi: 10.23919/ECC.2009.7074790.

Szimandl, B. and Nemeth, H. (2014). Robust servo control design for an electro-pneumatic clutch system using the hmethod. In *2014 IEEE/ASME 10th International Conference on Mechatronic and Embedded Systems and Applications (MESA)*, 1–6. doi: 10.1109/MESA.2014.6935526.

Szimandl, B. and Nemeth, H. (2013a). Dynamic hybrid model of an electro-pneumatic clutch system. *Mechatronics*, 23(1), 21 – 36. doi: https://doi.org/10.1016/j.mechatronics.2012.10.006.

Szimandl, B. and Nemeth, H. (2013b). Sliding mode position control of an electro-pneumatic clutch system. *IFAC Proceedings Volumes*, 46(2), 707 – 712. doi:https://doi.org/10.3182/20130204-3-FR-2033.00019. 5th IFAC Symposium on System Structure and Control.

XiaoJun, L., ChengRui, Z., HongBin, L., and XinLiang, W. (2006). Electronic pneumatic clutch control of the heavy truck based on neural network pid. In *2006 IEEE International Conference on Vehicular Electronics and Safety*, 232–235. doi:10.1109/ICVES.2006.371589.